LA-UR- 03-7719

Title: Detector tests for a prototype Compton imager

Author(s): John P. Sullivan, Gaetano Arnone, David K. Hayes, Andrew Hoover, R. Marc Kippen, Mohini W. Rawool-Sullivan, and Vern Sandberg

Los Alamos
NATIONAL LABORATORY

Detector tests for a prototype Compton imager

John P. Sullivan, Gaetano Arnone, David K. Hayes, Andrew Hoover, R. Marc Kippen, Mohini W. Rawool-Sullivan *Member, IEEE*, and Vern Sandberg

Abstract-- Compton imaging, which reconstructs the direction of incident photons based on the kinematics of Compton scattering, is of interest in the fields of astrophysics, medical imaging, and homeland defense. We are attempting to build a device in which the Compton scatter takes place in one of several layers of thin Silicon detectors and the secondary photon is detected in an array of high resolution photon detectors. We have purchased prototypes for both detector systems. This paper presents performance results from simulations and tests of the detectors.

I. INTRODUCTION

Development of technologies for detecting and characterizing radiation from various nuclear materials is important for many fields, including astrophysics, medical imaging, and homeland defense. Unfortunately, in many cases we now largely use the same detection technologies that were developed in the 1960s. While sufficient for some purposes, these technologies have proved inadequate for remote sensing of radioactive nuclear materials — a crucial capability required for enhanced homeland security as well as basic scientific advancement in astrophysics and planetary exploration. Passive gamma-ray detection is the most direct means of providing this capability, but current detectors are severely limited in sensitivity and detection range due to confusion from off-source backgrounds, and they cannot precisely localize sources when they are detected.

With the construction of our prototype we expect to develop new techniques that will produce passive gamma-ray detectors capable of localizing sources and rejecting backgrounds from irrelevant directions — thereby providing the improved sensitivity needed for remote nuclear material sensing. In addition we also intend to explore identification of shielded neutron sources and shielded material (by detecting gamma-rays originated from neutron activation of the shielding material) at close distances. The core technique to accomplish this goal is Compton imaging, which is based on the fact that Compton scattering (scattering of a gamma ray from an electron) preserves information about the direction and energy of incident gamma rays if the scattering byproducts can be precisely measured. Past attempts at Compton imaging suffered from the inability to perform these measurements with sufficient precision and efficiency, and by insufficient modeling and analysis capability to reconstruct the complex signals.

II. DETECTOR TECHNOLOGIES AND PROTOTYPE DETECTOR

Central to the design of a Compton imager is the choice of component detector technologies. There are two driving requirements: (1) an efficient scattering detector, where the primary recoil electron (and any secondary interactions of the scattered photons) can be tracked with reasonable accuracy, and (2) an absorbing detector to efficiently measure the full energy and direction of the scattered photon(s).

For the scattering detectors, a low-Z, low-density material is required to minimize Coulomb scattering and thereby enable electron tracking. Even if electron tracking is not employed, however, low-Z detectors are still required to minimize Doppler ambiguities in the Compton scatter reconstruction [1]. (Target electrons have non-zero bound orbital momentum that introduces uncorrectable uncertainties into the kinematic reconstruction, resulting in additional angular blur. This effect worsens with increasing Z of the scattering medium.) In addition, there must be a sufficient total thickness of active material to achieve reasonable detection efficiency. Gas detectors, for example, could provide good electron tracking capability, but they must be impractically thick (several meters) to yield reasonable detection efficiency. Furthermore,

John P. Sullivan is with the Los Alamos National Lab, P-25, MS-H846, Los Alamos, NM 87545 USA (telephone: 505-665-5963, e-mail: sullivan@lanl.gov).

Gaetano Arnone is with the Los Alamos National Lab, N-2, MS-J562, Los Alamos, NM 87545 USA (telephone: 505-667-0577, e-mail: garnone@lanl.gov).

David K. Hayes is with the Los Alamos National Lab, N-2, MS-J562, Los Alamos, NM 87545 USA (telephone: 505-67-4523, e-mail: dkhayes@lanl.gov).

Andrew Hoover is with the Los Alamos National Lab, ISR-2, MS-D436, Los Alamos, NM 87545 USA (telephone: 505-664-0979, e-mail: ahoover@lanl.gov).

R. Marc Kippen is with the Los Alamos National Lab, ISR-2, MS-B244, Los Alamos, NM 87545 USA (telephone: 505-667-3125, e-mail: mkippen@lanl.gov).

Mohini W. Rawool-Sullivan is with the Los Alamos National Lab, N-2, MS-B228, Los Alamos, NM 87545 USA (telephone: 505-667-6628, e-mail: mohini@lanl.gov).

Vern Sandberg is with the Los Alamos National Lab, ISR-2, MS-B244, Los Alamos, NM 87545 USA (telephone: 505-667-7268, e-mail: sandberg@lanl.gov).

the best gas detectors use xenon, which at Z = 54 results in significant Doppler angular blur. We therefore choose solid-state silicon detectors for the scattering medium.
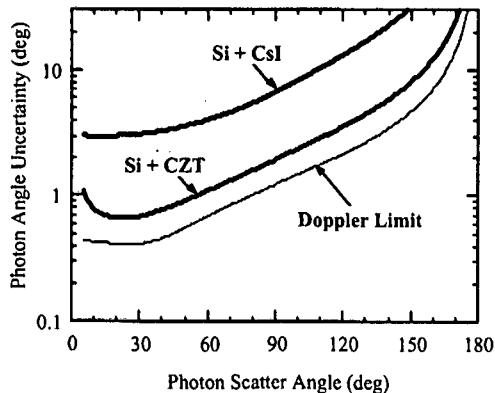

Fig. 1. Predicted scatter-angle resolution of Compton imagers using silicon scattering detectors and either CsI or CZT absorbing detectors (1 MeV incident gamma rays). Note that CZT, with its better position and energy resolution, performs near the physical Doppler limit.

At present, silicon is the only detection medium where recoil electron tracking has been amply demonstrated (need references). A stack of many thin silicon detectors simultaneously provides good detection efficiency and electron tracking capability. For a fixed number of readout channels, the choice of layer thickness is a tradeoff [2] between electron tracking precision (where thinner is better), detection efficiency (where thicker is better), and ruggedness (where thicker is better). In our prototype, there are three Silicon detector planes. Each Silicon plane consists of a 16x20 array of 3mm x 3mm Silicon pads -- resulting in an active area of 4.8 x 6.0 cm in each plane. The detectors are 300 microns thick. The readout system for the Silicon is a custom-designed and built system from IDE, based on their VA/TA preamp/trigger chip combination, and controlled by their VA-DAQ data acquisition system.

For the absorbing detectors, a high-Z, high-density detector with good energy and spatial resolution is required to precisely measure the full energy and direction of the Compton scattered photon(s). Segmented scintillators such as CsI(Tl) are being developed for this purpose [3] [4] but their marginal energy and spatial resolution severely limits imaging system performance (see Fig. 1). To achieve optimum system performance, millimeter spatial resolution and few-percent energy resolution are required. Due to Doppler broadening, further improvements in detector performance do not yield significant imaging enhancements. Position-sensitive germanium detectors are one option being investigated [5], but germanium detectors must be operated at cryogenic temperatures, making them problematic for use in space experiments or ground-based emergency response applications. Cadmium zinc telluride (CZT) detectors will

provide the needed performance at room temperature. But even to this date it is difficult to obtain large number of good quality CZT detectors. The price is also a driving concern along with the time constraint under which this prototype is being constructed. Fig. 1, shows that the imaging performance with CZT as an absorbing detector is expected to be near the Doppler limit if ~1-mm spatial resolution can be achieved. Even though we believe that an improved absorbing detector is the single most important development that can be made to enhance imaging performance, we chose a CsI/PIN array as an absorbing detector for our prototype due to is availability and reduced cost. Each CsI/PIN detector of the array is ~ 12 x 14 x10 mm in size. Individual detectors are arranged in a 6 x 7 detector array whose front face covers ~ 84 x 86 mm. The CsI detectors were built by St. Gobain, which also supplied photo-diodes + charge-sensing preamps for each channel.
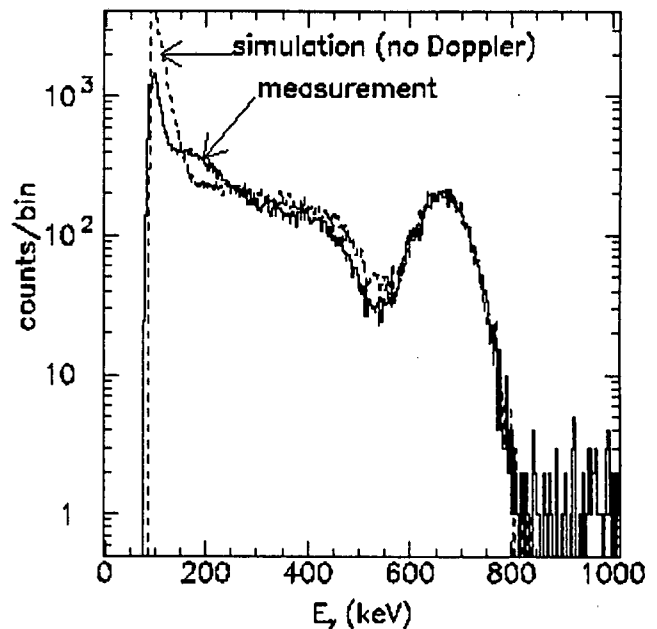

Fig. 2. Comparison of measured and simulated response of a single CsI detector from the prototype to a 662 MeV gamma-ray. Doppler broadening is not included in the simulation.

III.CsI/PIN DIODE ARRAY TESTS

We have not yet purchased a readout system for the complete CsI array. However, each individual detector has been tested using a shaping amplifier and a pulse-height analyzer. The individual crystals were tested with various gamma-ray sources. Fig. 2 shows a sample of the response of an individual crystal to 662 keV photons from a ^{137}Cs source. The measurement is compared to a result from a GEANT3 [6] simulation of the detector with an assumed resolution of 47 keV (sigma), independent of measured energy. The assumed resolution was adjusted to agree with the observed width of the full energy photon peak. The simulation in Fig. 2 does not include Doppler broadening. Fig. 3 compares the same measurement with the same simulation, except that Doppler

broadening (based on the GLECS package [7]) is included in the simulation. The addition of Doppler broadening to the simulation seems to improve the agreement with the data in the "valley" between the full energy photon peak (~662 keV) and the Compton edge (~450 keV). The resolutions of the other detectors in the array are similar to this sample detector. The resolution is sensitive to the temperature of the readout electronics – as a result we are building a simple air-cooling system to improve the resolution.
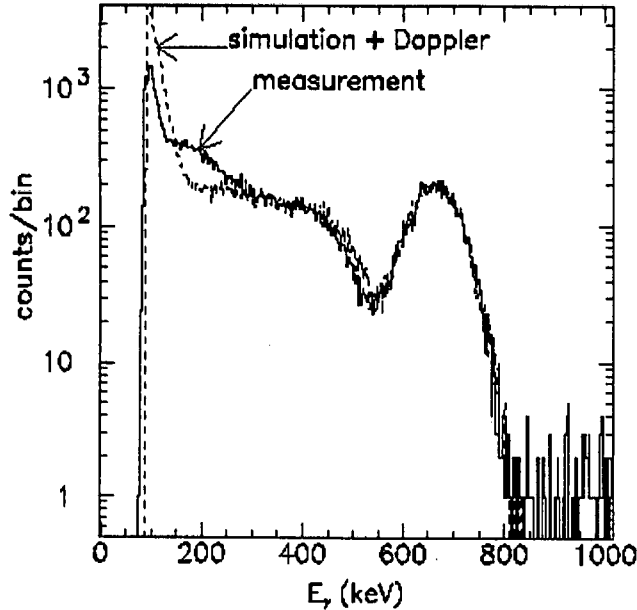

Fig.3. Comparison of measured and simulated response of a single CsI detector from the prototype to a 662 MeV gamma-ray. Doppler broadening is included in the simulation.

IV. SILICON DETECTOR TESTS

The noise in the Silicon detector + readout electronics system consists of both common-mode noise and an uncorrelated noise component. For the electronics alone, before connecting the Silicon detectors, the common-mode noise is estimated to be equivalent to approximately 1 keV (rms) of photon energy loss and the uncorrelated noise is about 0.5 keV (about 130 electrons equivalent). Because there are very few hits per event in the silicon, the common mode noise can be safely subtracted – so the uncorrelated noise is the most relevant number. When the Silicon detectors are attached, the uncorrelated noise increases to approximately 2.6 keV (720 electrons equivalent). These noise estimates are close to our expectations, but are based on a calibration using the charge injected from an internal calibration system in the readout electronics. We have not yet confirmed this calibration with an external calibration source.
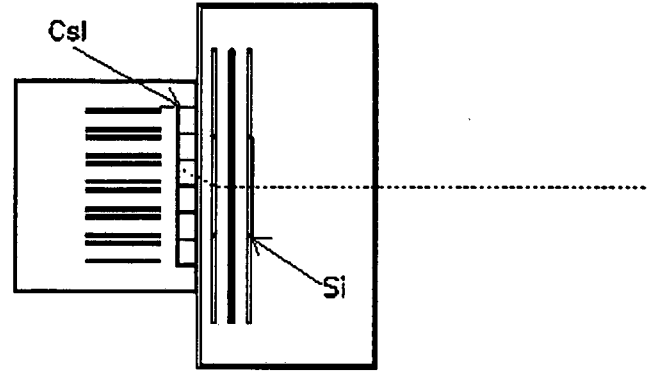

Fig. 4. A cross-section of the simulated detector system. The CsI detectors are shown by the small rectangles marked by an arrow. One of the circuit boards holding the Silicon Pad detectors are also marked with an arrow. The Silicon detectors are smaller than the circuit boards. The dotted line shows a 662 keV photon coming from the right.

V. SIMULATED IMAGE RECONSTRUCTION

A simple image reconstruction algorithm was written. This algorithm has been used to try to reconstruct the true location of the image in an idealized case. In the simulations, the Silicon detectors were arrayed in three parallel planes, separated by 1 cm. The closest Silicon plane was positioned 1 cm from the front face of the CsI array.

Fig. 4 shows a sketch of the (GEANT3) detector model. The dotted line indicates a 662 keV photon entering the detector system from the right and Compton scattering in the third Silicon layer. The resulting electron is stopped in the same Silicon layer. The scattered photon is absorbed in a CsI detector. The model includes most of the passive material in the system such as circuit boards for readout (the narrow rectangles to the left of the CsI detectors represent the CsI preamp boards) and the boxes containing the detectors. The sample event below shows the initial photon pointed directly along the "z" axis at x=0, y=0, where the z axis is defined as the central axis of the Silicon detectors and the CsI array. The initial z position is 25 cm from the front face of the CsI array. In the simulations used to try to reconstruct the source location, the simulated source was placed at various values of x and y. The 662 keV photons were emitted isotropically.

The output from the Geant simulation was a list of energies deposited in each detector element for each event. We have written a set of algorithms which attempt to reconstruct the location of the source from the simulated data. In the reconstruction phase, the resolution of the Silicon detectors was assumed to be 5 keV (sigma) and the resolution of the CsI detectors was assumed to be 50 keV (sigma). These simulated "data" were then reconstructed using a set of simple algorithms.

The algorithms take each combination of one hit in the CsI and one hit in the Silicon and assume it is from a Compton scatter event. The opening angle and direction of the "cone"

which is reconstructed from the event is calculated. These cones are then projected onto a set of planes perpendicular to the z axis at various distances from the detector. Rather than calculate the intersection of the cones with each plane, a series of 100 vectors, equally spaced azimuthally around the cone, are projected onto each plane. The "planes" are represented by two-dimensional histograms. Figure 5 shows the sample rings for 10 events (and "event" means there was at least one hit in both the Silicon and in the CsI). The horizontal and vertical lines show the true source location – at x=0, y=0 in this case. This plane is selected to be at the true z position of the source. The various rings tend to intersect near the true location of the source – but they typically miss the true source location by 5-10 cm. The rings miss the correct location in and y for several reasons. Among the reasons are the resolution of the detector (especially the CsI) and the fact that many of the reconstructed events are not simple Compton scatter events. In constructing Fig. 5, we attempted to enhance the fraction of true Compton scatter events in the sample by using only those events with exactly one hit in the CsI and one hit in the Silicon.
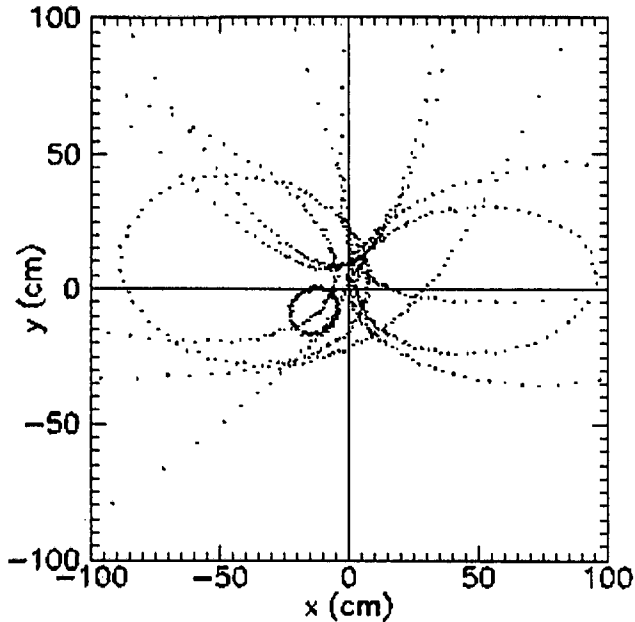

Fig. 5. A set of example "rings" for a ten events. The horizontal and vertical lines represent the true location of the source – at x=0, y=0 in this case. This plane is selected to be at the z position of the true source.

When many millions of simulated events are added into a histogram like the one show in Fig. 5, the expectation is that the correct source location will appear as a peak in the two-dimensional histogram. We have done a series of these simulations for different x and y source locations. Fig. 6 shows a cut along the x axis through one such two-dimensional histogram. This cut is taken at the y value corresponding to the maximum in the two-dimensional histogram. In this case, the source was at x = 5 cm and y = -2 cm. The peak in the two dimensional histogram was found at x = 3.5+-0.5 and y = -0.5+-0.5, where the +-0.5 terms indicated the size of the bin (1 cm) in the two-dimensional histogram. In fig. 6, the arrow

marks the true source location in x. The actual peak is seen slightly below the true value.
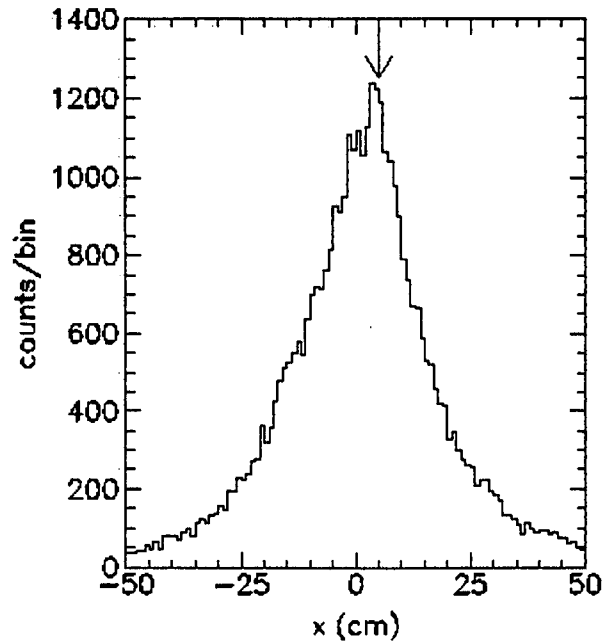

Fig. 6. A plot of the x distribution of "hits" for the value of the y position corresponding to the peak in the 2D distribution. The arrow marks the true x position of the source.

Tests with a number of source locations have shown that the source position found by this reconstruction algorithm is systematically closer to x=0, y=0 that the true source location.

VI. CONCLUSIONS

We plan to purchase electronics to complete the readout system for the CsI. We also plan to work on the resolution of the CsI, notably by reducing and stabilizing the temperature of the photodiodes and preamps. We also plan to simulate more realistic sources, including background, and to improve our reconstruction algorithms. The next major step will be to take data with a complete readout system and compare it to simulations. Validating out simulations will be a key step towards the construction of a larger operational device.

The data shown in Fig. 6 come from a total of 4.8×10^8 ^{137}Cs decays – corresponding to about 21 minutes for a typical 10 uCi (3.7×10^5 Bq) source. The desire for larger detectors, better resolution, and better algorithms is clear.

VII. REFERENCES

[1] C. E. Ordonez, A. Bolozdynya, W. Chang, "Doppler broadening of energy spectra in Compton cameras," *IEEE Nucl. Sci. Symp. Conf. Record, vol 2*, pp. 1361 (1997).

[2] M. W. Rawool-Sullivan, J. P. Sullivan, J. E. Koster, and B. D. Rooney, "Validity and Limitations of the Three-Plane Compton Imaging Technique via Simulations," *IEEE Trans. Nucl. Sci., 49(6)*, pp. 3290-3294, Dec. 2002.

[3] O. T. Tumer *et al.*, "The TIGRE instrument for 0.3-100 MeV gamma-ray astronomy," *IEEE Trans. Nucl. Sci. 42(4)*, pp. 907-916, Aug. 1995.

[4] G. Kanbach et al., "Concept study for the next generation medium-energy gamma-ray astronomy mission: MEGA," Proc. SPIE 4851, 1209 (2003).

[5] B. F. Philips et al., "Development of germanium strip detectors for environmental remediation," *IEEE Trans. Nucl. Sci. 49(2)*, pp. 597-600, Apr. 2002.

[6] GEANT – Detector description and simulation tool, available online at: http://www.asd.web.cern.ch/wwwasd/geant/

[7] R. M. Kippen, GLECS and GLEPS – GEANT3 low-energy Compton scattering packages, available online at: http://nis-www.lanl.gov/~mkippen/actsim/glecs/